

Compendium of Single Event Effects, Total Ionizing Dose, and Displacement Damage for Candidate Spacecraft Electronics for NASA

Kenneth A. LaBel, Martha V. O'Bryan, Dakai Chen, Michael J. Campola, Megan C. Casey, Jonathan A. Pellish, Jean-Marie Lauenstein, Edward P. Wilcox, Alyson D. Topper, Raymond L. Ladbury, Melanie D. Berg, Robert A. Gigliuto, Alvin J. Boutte, Donna J. Cochran, Stephen P. Buchner, and Daniel P. Violette

Abstract--We present results and analysis investigating the effects of radiation on a variety of candidate spacecraft electronics to proton and heavy ion induced single event effects (SEE), proton-induced displacement damage (DD), and total ionizing dose (TID). This paper is a summary of test results.

I. INTRODUCTION

NASA spacecraft are subjected to a harsh space environment that includes exposure to various types of ionizing radiation. The performance of electronic devices in a space radiation environment is often limited by its susceptibility to single event effects (SEE), total ionizing dose (TID), and displacement damage (DD). Ground-based testing is used to evaluate candidate spacecraft electronics to determine risk to spaceflight applications. Interpreting the results of radiation testing of complex devices is quite difficult. Given the rapidly changing nature of technology, radiation test data are most often application-specific and adequate understanding of the test conditions is critical [1].

Studies discussed herein were undertaken to establish the application-specific sensitivities of candidate spacecraft and emerging electronic devices to single-event upset (SEU), single-event latchup (SEL), single-event gate rupture (SEGR), single-event burnout (SEB), single-event transient (SET), TID, enhanced low dose rate sensitivity (ELDRS), and DD effects.

Manuscript received July 30, 2014 This work was supported in part by the NASA Electronic Parts and Packaging Program (NEPP), NASA Flight Projects, and the Defense Threat Reduction Agency (DTRA).

Kenneth A. LaBel, Dakai Chen, Michael J. Campola, Megan C. Casey, Jonathan A. Pellish, Jean-Marie Lauenstein, Raymond L. Ladbury, Alvin J. Boutte, and Daniel P. Violette are with NASA/GSFC, Code 561.4, Greenbelt, MD 20771 (USA), phone: 301-286-9936, emails: kenneth.a.label@nasa.gov, Dakai.Chen-1@nasa.gov, michael.j.campola@nasa.gov, megan.c.casey@nasa.gov, jonathan.a.pellish@nasa.gov, jean.m.lauenstein@nasa.gov, raymond.l.ladbury@nasa.gov, Alvin.J.Boutte@nasa.gov, Daniel.P.Violette@nasa.gov.

Martha V. O'Bryan, Edward P. Wilcox, Alyson D. Topper, Melanie D. Berg, and Robert A. Gigliuto are with AS&D, Inc. (ASRC Federal Space and Defense), 7515 Mission Drive, Suite 200, Seabrook, MD 20706, work performed for NASA Goddard Space Flight Center (GSFC), emails: martha.v.obryan@nasa.gov, Ted.Wilcox@nasa.gov, Alyson.D.Topper@nasa.gov, Melanie.D.Berg@nasa.gov, Robert.A.Gigliuto@nasa.gov, and Donna.J.Cochran@nasa.gov.

Stephen P. Buchner is with Naval Research Laboratory, email: buchner@ccs.nrl.navy.mil.

II. TEST TECHNIQUES AND SETUP

A. Test Facilities

All tests were performed between February 2013 and February 2014. Heavy ion experiments were conducted at the Lawrence Berkeley National Laboratory (LBNL) [2] and at the Texas A&M University Cyclotron (TAMU) [3]. Both of these facilities are suitable for providing a variety of ions over a range of energies for testing. The devices under test (DUTs) were irradiated with heavy ions having linear energy transfers (LETs) ranging from 0.6 to 120 MeV•cm²/mg. Fluxes ranged from 1x10² to 1x10⁵ particles/cm²/s, depending on device sensitivity. Table 1 shows representative ions used at LBNL and Table 2 contains representative ions used at TAMU. LETs in addition to the values listed were obtained by changing the angle of incidence of the ion beam with respect to the DUT, thus changing the path length of the ion through the DUT and the "effective LET" of the ion [4]. Energies and LETs available varied slightly from one test date to another.

Laser SEE tests were performed at the pulsed laser facility at the Naval Research Laboratory (NRL) using two-photon absorption [5], [6] with the light incident from the back side of the wafer following polishing to produce a mirror-like finish. The laser light parameters are listed in Table III.

Proton SEE, DD and TID tests were performed at the University of California at Davis (UCD) Crocker Nuclear Laboratory (CNL) using a 76" cyclotron (maximum energy of 63 MeV) [7]. Pulse width and beam spot size are listed in Table IV.

TID testing was performed using a ⁶⁰Co source. The source is capable of delivering dose rates between 0.0005 rad(Si)/sec and 50 rad(Si)/sec.

TABLE I: LBNL TEST HEAVY IONS

Ion	Energy (MeV)	Surface LET in Si (MeV·cm ² /mg) (Normal Incidence)	Range in Si (μm)
¹⁸ O	183	2.2	226
²² Ne	216	3.5	175
⁴⁰ Ar	400	9.7	130
²³ V	508	14.6	113
⁶⁵ Cu	660	21.2	108
⁸⁴ Kr	906	30.2	113
¹⁰⁷ Ag	1039	48.2	90
¹²⁴ Xe	1233	58.8	90
LBNL 10 MeV per amu tune			

TABLE II: TAMU TEST HEAVY IONS

Ion	Energy (MeV)	Surface LET in Si (MeV·cm ² /mg) (Normal Incidence)	Range in Si (μm)
¹⁴ N	210	1.3	428
²⁰ Ne	300	2.5	316
⁴⁰ Ar	599	7.7	229
⁶³ Cu	944	17.8	172
⁸⁴ Kr	1259	25.4	170
¹⁰⁹ Ag	1634	38.5	156
¹²⁹ Xe	1934	47.3	156
¹⁹⁷ Au	2954	80.2	155
TAMU 15 MeV per amu tune			
⁸⁴ Kr	2081	19.8	332
¹³⁹ Xe	3197	38.9	286
TAMU 25 MeV per amu tune			

amu = atomic mass unit

TABLE III: LASER TEST FACILITY

Naval Research Laboratory (NRL) Pulsed Laser SEE Test Facility Laser: 1260 nm, 140 fs pulse width, beam spot size ~1.3 μm and repetition rate of 1 KHz.
--

TABLE IV: PROTON TEST FACILITIES

University of California at Davis (UCD) Crocker Nuclear Laboratory (CNL), energy tunes ranged from 6.5 to 63 MeV, flux ranged from 8×10^7 to 1×10^9 particles/cm ² /s.

B. Test Method

Unless otherwise noted:

All tests were performed at room temperature and with nominal power supply voltages. We recognize that temperature effects and worst-case power supply conditions are recommended for device qualification; SEE testing was performed in accordance with JESD57 test procedures [8]; and TID testing was performed in accordance with MIL-STD-883, Test Method 1019 [9].

1) SEE Testing - Heavy Ion:

Depending on the DUT and the test objectives, one or more of three SEE test methods were typically used:

Dynamic – the DUT was exercised continually while being exposed to the beam. The events and/or bit errors were counted, generally by comparing the DUT output to an unirradiated reference device or other expected output (Golden chip or virtual Golden chip methods) [10]. In some cases, the effects of clock speed or device operating modes were investigated. Results of such tests should be applied with caution due to the application-specific nature of the results.

Static – the DUT was configured prior to irradiation; data were retrieved and errors were counted after irradiation.

Biased – the DUT was biased and clocked while power consumption was monitored for SEL or other destructive effects. In most SEL tests, functionality was also monitored.

In SEE experiments, DUTs were monitored for soft errors, such as SEUs, and for hard errors, such as SEGR. Detailed descriptions of the types of errors observed are noted in the individual test reports [11], [12].

SET testing was performed using high-speed oscilloscopes controlled via LabVIEW®. Individual criteria for SETs are specific to the device and application being tested. Please see the individual test reports for details [11], [12].

Heavy ion SEE sensitivity experiments include measurement of the linear energy transfer threshold (LET_{th}) and cross section at the maximum measured LET. The LET_{th} is defined as the maximum LET value at which no effect was observed at an effective fluence of 1×10^7 particles/cm². In the case where events are observed at the smallest LET tested, LET_{th} will either be reported as less than the lowest measured LET or determined approximately as the LET_{th} parameter from a Weibull fit. In the case of SEGR experiments, measurements are made of the SEGR threshold V_{ds} (drain-to-source voltage) as a function of LET and ion energy at a fixed V_{gs} (gate-to-source voltage).

2) SEE Testing - Proton

Proton SEE tests were performed in a manner similar to heavy ion exposures. However, because protons cause SEE via indirect ionization of recoil particles, results are parameterized in terms of proton energy rather than LET. Because such proton-induced nuclear interactions are rare, proton tests also feature higher cumulative fluences and particle flux rates than heavy ion experiments.

3) SEE Testing - Pulsed Laser

DUTs are mounted on an X-Y-Z stage that can move in steps of 0.1 microns for accurate determination of the volumes sensitive to single event effects. The light is incident from the back side, which is polished to a mirror-like finish, and is focused through the substrate using a 100x lens that produces a spot diameter of approximately 1.3 μm at full-width half-maximum (FWHM). An illuminator, together with an infrared camera and monitor, were used to image the area of interest thereby facilitating accurate positioning of the device in the beam. The pulse energy was varied in a continuous manner using a polarizer/half-waveplate combination and the energy was monitored by splitting off a portion of the beam and directing it at a calibrated energy meter.

4) TID Testing - ^{60}Co

The test procedures, including the radiation dosimetry details, are most often performed in accordance with the latest version of MIL-STD-883 Test Method 1019 [9]. Unless otherwise noted, the irradiation was performed using a room in-air ^{60}Co facility where the sources are raised up out of the floor during exposures. Active dosimetry was performed using air ionization probes. The DUTs were placed inside a standard Pb/Al filter box.

5) Displacement Damage - Proton Testing

Proton-induced displacement damage tests were performed on biased devices. Functionality and parametric changes were measured either continually during irradiation (in-situ) or after step irradiations (for example: every 10 krad(Si), or every 1×10^{10} protons/cm 2).

III. TEST RESULTS OVERVIEW

Principal investigators are listed in Table V. Abbreviations and conventions are listed in Table VI. SEE results are summarized in Table VII. Unless otherwise noted all LETs are in MeV \cdot cm 2 /mg and all cross sections are in cm 2 /device. All SEL tests are performed to a fluence of 1×10^7 particles/cm 2 unless otherwise noted.

TID and DD results are summarized in Table VIII and a synopsis of low dose rate on-going TID results are in Table IX.

TABLE V: LIST OF PRINCIPAL INVESTIGATORS

Principal Investigator (PI)	Abbreviation
Melanie D. Berg	MB
Megan C. Casey	MCC
Michael J. Campola	MJC
Dakai Chen	DC
Robert A. Gigliuto	RG
Raymond L. Ladbury	RL
Jean-Marie Lauenstein	JML
Jonathan A. Pellish	JP

TABLE VI: ABBREVIATIONS AND CONVENTIONS

LET = linear energy transfer (MeV \cdot cm 2 /mg)
LET $_{th}$ = linear energy transfer threshold (the maximum LET value at which no effect was observed at an effective fluence of 1×10^7 particles/cm 2 – in MeV \cdot cm 2 /mg)
< = SEE observed at lowest tested LET
> = no SEE observed at highest tested LET
σ = cross section (cm 2 /device, unless specified as cm 2 /bit)
σ_{max} = cross section at maximum measured LET (cm 2 /device, unless specified as cm 2 /bit)
amu = atomic mass unit
Ag = Silver
Ar = Argon
A $_{VO}$ = open loop gain
BiCMOS = bipolar complementary metal oxide semiconductor
CCD = charge coupled device
CMOS = complementary metal oxide semiconductor
DIMM = dual inline memory module
DUT = device under test
EF = enhancement factor
ELDRS = enhanced low dose rate sensitivity
FF = functional failure
H = heavy ion test
h $_{FE}$ = forward current gain
ID# = identification number
I $_{IB}$ = input bias current
I $_{out}$ = output current
L = laser test
LBNL = Lawrence Berkeley National Laboratory
LDC = lot date code
LDMOS = laterally diffused metal oxide semiconductor
LDR = low dose rate
LVPECL = Low-voltage positive emitter-coupled logic
MOSFET = metal-oxide-semiconductor field-effect transistor
NA = not available
NAND = Negated AND or NOT AND
NRL = Naval Research Laboratory
PI = principal investigator
REAG = radiation effects and analysis group
ReRAM = Reduction-oxidation random access memory
Rev. = revision
RX = receiver output
SEB = single event burnout
SEE = single event effect
SEGR = single event gate rupture
SEL = single event latchup
SET = single event transient
SEU = single event upset
Si = Silicon
SiC = silicon carbide
SiGe = silicon germanium
SJ VDMOS = super junction vertical double diffused MOSFET
SOI = silicon on insulator
Ta = Tantalum
TAMU = Texas A&M University Cyclotron Facility
TO = transistor outline
TX = transceiver output
V = volt
V $_{BE}$ = base-emitter voltage
V $_{cc}$ = power supply voltage / core voltage
V $_{CE}$ = collector-emitter voltage
V $_{CM}$ = common mode voltage
V $_{DS}$ = drain-source voltage
V $_{GS}$ = gate-source voltage
V $_{IH}$ = input high voltage
V $_{IL}$ = input low voltage
V $_{IH_min}$ = input low minimum voltage
V $_{IL_max}$ = input low maximum voltage
V $_{in}$ = input voltage
V $_{IO}$ = input/output voltage
V $_{OS}$ = input offset voltage
V $_{OUT}$ = output voltage
V $_R$ = reverse voltage
Xe = Xenon

TABLE VII: SUMMARY OF SEE TEST RESULTS

Part Number	Manufacturer	LDC or Wafer #; REAG ID#	Device Function	Technology	Particle: (Facility/Year/Month) P.I.	Test Results: LET in MeV·cm ² /mg, σ in cm ² /device, unless otherwise specified	Supply Voltage	Sample Size (Number Tested)
Logic Device:								
ACT4468	Aeroflex	1210; 13-039	Transceiver	Bipolar	H: (TAMU13May) DC	SET 2.8 < LET _{th} < 4.0 $\sigma_{max} = 7 \times 10^{-4}$ cm ² [13]	5 V	3
SNJ54LVC14AFK	Texas Instruments	1137B; 13-029	Hex Schmitt-Trigger Inverter	BiCMOS	H: (TAMU13May) DC	SEL _{th} ~ 70 $\sigma_{max} = 7 \times 10^{-6}$ cm ² at 100°C Not immediately destructive. [14]	3.5 V	3
SiC:								
GB20SLT12	GeneSiC	1209; 13-032	Schottky Diode	SiC	H: (TAMU13June) JML/MCC	Immediate catastrophic SEB at 500 V _R with 1110 MeV Ag. V _{RRM} and I _R severely degraded at lower V _R . 1110 MeV Ag: threshold for degradation < 350 V; 709 MeV Cu: < 375 V; 267 MeV Ne: 550 V < V _R < 600 V. [15]	Up to 1100 V _R	14
C4D40120D	CREE	Wafer # E23312; 13-033	Schottky Diode	SiC	H: (TAMU13May) MCC	1110 MeV Ag: SEE-induced degradation V _R < 150 V; V _R threshold for catastrophic failure (SEB) < 500 V. [16]	Up to 650 V _R	9
CPM-1200-0025B	CREE	1327; 13-069	Power MOSFET	SiC	H: (LBNL13Sept) MCC	996 MeV Xe: Immediate catastrophic SEB at V _{DS} < 650 V; threshold not found. At all other voltages tested, degradation in both gate and drain currents was observed suggestive of SEB damage. [17]	0 V _{GS}	8
MSK1852P	CREE (Packaged by MSKennedy)	1332; 13-070	Power MOSFET	SiC	H: (LBNL13Sept) MCC	At voltages up to 500 V _{DS} and at all beam conditions tested, no immediate catastrophic failure was observed but degradation in both gate and drain currents was observed. Failures were suggestive of SEGR damage. [18]	0 V _{GS}	13
MSK1852PN	CREE (Packaged by MSKennedy)	1332; 13-071	MOSFET	SiC	H: (LBNL13Sept) MCC	At all voltages and beam conditions tested, no immediate catastrophic failure was observed but degradation in both gate and drain currents were observed. Failures were suggestive of SEB damage. [19]	0 V _{GS}	11
CHTPLA8543C	Cissoid	1312; 1324; 13-044	Power MOSFET	SiC	H: (TAMU13June); H: (LBNL13Sept) JML	Contact PI for test results.	0 V _{GS}	8
IDW40G65C5FKSA1	Infineon	HAA249; 13-038	Schottky Diode	SiC	H: (TAMU13May-Jun) MCC	1289 MeV Ag: SEB induced degradation V _R < 200 V; immediate catastrophic failure observed at V _R = 300 V. [20]	Up to 300 V _R	13
Power:								
IPW65R019C7	Infineon	HAA249; 13-060	MOSFET	SJ VDMOS	H: (TAMU13June) JML	SEB. 1289 MeV Ag: 300 V < V _{DS} < 325 V [21]	0 V _{GS}	3
MOS-250-2	FUJI	Test Chip; 13-061	MOSFET	VDMOS	H: (LBNL13Sept) JML	SEGR. 1233 MeV Xe (LET = 59) pass 250 V _{DS} at 0 to -10 V _{GS} ; fail < 200 V _{DS} at -15 V _{GS} . [22]	0, -10, -15 V _{GS}	3
B1230-X18, CA18HA	JAZZ	Test Chip; A613	MOSFET	LD MOS	H: (TAMU13June); (LBNL13Sept) JML	Contact PI for test results.	0 V _{GS}	N/A
IXDI630CI	IXYS	1209; 13-034	MOSFET Gate Driver	CMOS	H: (TAMU13June) MCC	SEL 8.6 < LET _{th} < 20. [23]	35 V	4
ADUM3223AR7	Analog Devices	1251; 13-031	Half-Bridge, Driver	CMOS	H: (TAMU13May) MCC	SEL LET _{th} < 8.3. [24]	5 V	3
Memory:								
K4T1G084QF-BCE6 die on M470T2863FB3-CE6 DIMM	Samsung	LDC NA; 12-036	DDR2	CMOS	L: (NRL14Jan) RL	SEU were seen when the DDR2 memory array was irradiated with laser at NRL two-photon absorption facility. [25]	1.5 V	1

Part Number	Manufacturer	LDC or Wafer #; REAG ID#	Device Function	Technology	Particle: (Facility/Year/Month) P.I.	Test Results: LET in MeV·cm ² /mg, σ in cm ² /device, unless otherwise specified	Supply Voltage	Sample Size (Number Tested)
K4B2G0846-HCH9 (13-015) 2 Gb die on M471B5773DH0-CH9 DIMMs and K4B4G0846B-HCH9 (12-037) 4Gb die on M471B5773DH0-CH9 DIMMs	Samsung	LDC NA; 13-015; 12-037	DDR3	CMOS	H: (TAMU13May) RL; L: (NRL13Mar) RL	H: SEU and SEFI seen down to lowest test 1.5 < LET > 2.5; Onset LET for block errors ~5; Onset LET for SEFI ~ 2. $\sigma_{\max} \sim 8 \times 10^{-4}$ cm ² per device for SEU, $\sim 1 \times 10^{-4}$ cm ² per device for block errors and $\sim 1 \times 10^{-5}$ cm ² per device SEFI. Die revision variance in stuck bit susceptibility, see test report. [26] L: No SEU were observed.	1.5 V	4 parts tested, 2 Rev. C die and 2 Rev. D die
MN101L	Panasonic	LDC NA; 13-075	Embedded Resistive Memory	ReRAM, 180 nm CMOS	H: (TAMU13Dec) DC	H: ReRAM array is immune to upsets. SEFI LET _{th} ~ 3.1; $\sigma = 4 \times 10^{-5}$ cm ² /device at LET of 70. [27]	3.3 V	3
Schottky Diodes:								
120720A	Crane Aerospace & Electronics	Wafer # 1-T33; 12-078	Schottky Diode	Si	H: (TAMU13May) MCC	No failures observed at 100% of reverse voltage when irradiated with 2076 MeV Ta. [28]	45 V	4
1N5819UB1	STMicroelectronics	Wafer # 31244A; 13-035	Schottky Diode	Si	H: (TAMU13June) MCC	No failures observed at 100% of reverse voltage when irradiated with 1512 MeV Xe. [28]	45 V	3
95-9942U	International Rectifier/Vishay	Wafer # 23; 13-048	Schottky Diode	Si	H: (TAMU13June) MCC	No failures observed at 100% of reverse voltage when irradiated with 1512 MeV Xe. [28]	150 V	3
95-9951U	International Rectifier/Vishay	Wafer # 7; 13-047	Schottky Diode	Si	H: (TAMU13June) MCC	No failures observed at 100% of reverse voltage when irradiated with 1366 MV Xe. [28]	45 V	3
95-9953U	International Rectifier/Vishay	Wafer # 320; 13-049	Schottky Diode	Si	H: (TAMU13June) MCC	No failures observed at 67% of reverse voltage when irradiated with 1512 MeV Xe. [28]	150 V	1
96-1052U	International Rectifier/Vishay	Wafer # 1; 13-046	Schottky Diode	Si	H: (TAMU13June) MCC	No failures observed at 100% of reverse voltage when irradiated with 1366 MeV Xe. [28]	60 V	3
96-1063U	International Rectifier/Vishay	Wafer # 4; 13-045	Schottky Diode	Si	H: (TAMU13June) MCC	No failures observed at 100% of reverse voltage when irradiated with 1366 MeV Xe. [28]	45 V	4
STPS1045CS1FR	STMicroelectronics	wafer 31203A; 13-036	Schottky Diode	Si	H: (TAMU13June) MCC	No failures observed at 100% of reverse voltage when irradiated with 1512 MeV Xe. [28]	45 V	3
STPS20100CFSY1FR	STMicroelectronics	wafer 31013A; 13-037	Schottky Diode	Si	H: (TAMU13May) MCC	Electrical characteristic degradation at 100% of rated voltage when irradiated with 1512 MeV Xe. Immediate catastrophic failure with 2076 MeV Ta. [28]	100 V	3
FPGA:								
Virtex 5QV	Xilinx	1217; 12-003 12-004	Virtex 5 FPGA	CMOS	H: (TAMU13May; June; Dec) MB	Contact PI for test results. [29]	4.5 V	2
A3PE3000L	Actel/Microsemi	1108; 12-052	ProASIC FPGA	CMOS	H: (TAMU13Dec) MB	Ongoing research investigating different mitigation strategies. [30] [31]	1.5; 2.5; and 3.3 V	2
Miscellaneous:								
IS2981	Intersil	0124; 13-043	Source driver	CMOS	H: (TAMU13May) DC	SET 15.3 < LET _{th} < 18.4 $\sigma_{\max} = 1 \times 10^{-3}$ cm ² [32]	28 V	3
LM6172	Texas Instruments	1208A; 13-076	Operational Amplifier	Bipolar	H: (TAMU13Dec) MCC	SET 0.14 < LET _{th} < 0.87 $\sigma_{\max} = 1 \times 10^{-3}$ cm ² [33]	±5 V	2
ADV212	Analog Devices	1216; 1220; 13-052; 13-053	Video Codec	Hybrid 0.18 μ CMOS	H: (TAMU13June) RG	SEL 1.3 < LET _{th} < 2.7; SEFI LET _{th} < 1.3; Frame Upsets LET _{th} < 1.3 [34]	1.5 V; 3.3 V	3

Part Number	Manufacturer	LDC or Wafer #; REAG ID#	Device Function	Technology	Particle: (Facility/Year/Month) P.I.	Test Results: LET in MeV·cm ² /mg, σ in cm ² /device, unless otherwise specified	Supply Voltage	Sample Size (Number Tested)
CMOS – Test Chip:								
32 nm SOI (Deneb)	IBM	Test Chip; 13-067	SET Pulse Width Measurement	32 nm SOI CMOS	H: (LBNL13Sept) JP	SET pulse width data gathered from 2-59 MeV·cm ² /mg. This was an initial test of the device; follow-up testing will be required to complete the data set. [35]	0.9 V	2
32nm SOI (Hogwarts)	IBM	2291, 2109; 2210; 12-033; A617	SRAM	32nm SOI	H: (LBNL13Jan; TAMU13May) JP; P: (UCD13Nov) JP	SRAM tested with the 10 MeV/amu cocktail at LBNL, the 25 MeV/amu tune at TAMU, protons from 64 MeV down to stopping at UCD, and alpha particles from 30 MeV down to stopping at UCD. $\sigma_{\max} \sim 1 \times 10^{-3}$ cm ² /Mbit with an SEU LET _{th} < 0.9. The SRAM was sensitive to low-energy protons. [36]	0.77 & 1.05 V	1

TABLE VIII: SUMMARY OF TID AND DD TEST RESULTS

Dose rate (mrad(Si)/s) or Proton Energy (MeV) unless otherwise specified.

Part Number	Manufacturer	LDC or Wafer #; REAG ID#	Device Function	Technology	PI	Results	App. Spec (Y/N)	Dose rate (mrad(Si)/s) or Proton Energy (MeV)	Degradation Level (krad(Si)) or Proton Fluence
Operational Amplifier:									
AD648	Analog Devices	1225; 13-005	Operational Amplifier	Bipolar	MCC	Input bias current and open loop gain out of spec between 20 and 30 krad(Si). Parts experienced functional failure between 70 and 80 krad(Si). [37]	N	10	20 < I _{IB} , A _{VO} < 30
OP471	Analog Devices	0646A; 13-010	Operational Amplifier	Bipolar	RL	All parameters within specifications up to 50 krad(Si); equipment failure led to VOS measurements being unusable [38]	Y	0.01 rad(Si)/s	>50 (V _{OS} data invalid)
OP484	Analog Devices	1039; 12-072	Operational Amplifier	Bipolar	RL	All parameters remained within specifications up to and including 15 krad(Si). VIO went out of specification between 15 and 20 krad(Si). All other parameters remained within specification to 40 krad(Si). [39]	Y	0.01 rad(Si)/s	15 < V _{IO} < 20
OP497	Analog Devices	1118A 13-041	Operational Amplifier	Bipolar	MJC	Input offset current out of spec >5 krad(Si). [40]	Y	10	4.5 < V _{CM} < 7
Transistor:									
SFT2369	Solid State Devices, Inc.	1047; 13-028	Transistor	Bipolar	DC	Gain degradation. No bias dependence. [41]	N	10	>50
SFT2907A	Solid State Devices, Inc.	1047; 13-027	Transistor	Bipolar	DC	Gain exceeded specifications. No bias dependence. [42]	N	10	20 < h _{FE} < 40
SFT2222A	Solid State Devices, Inc.	1046; 13-026	Transistor	Bipolar	DC	Gain exceeded specifications. Minimal bias dependence. [43]	N	10	30 < h _{FE} < 50
Analog/Linear:									
SMA1031	M/A-COM	1218; 12-051	Amplifier	Bipolar	MJC	All parameters remained in specification to 20 krad(Si). [44]	Y	10	>20
Miscellaneous:									
NB7L14MN	On Semiconductor	0936; 12-055	Differential 1:4 LVPECL Fanout Buffer	SiGe	MJC	All parameters remained in specification to 20 krad(Si). [45]	Y	10	>20

Part Number	Manufacturer	LDC or Wafer #; REAG ID#	Device Function	Technology	PI	Results	App. Spec (Y/N)	Dose rate (mrad(Si)/s) or Proton Energy (MeV)	Degradation Level (krad(Si)) or Proton Fluence
STAR1000	Cypress Semiconductor	1207; 13-042	CCD Image Sensor	CMOS	MJC	All parameters remained in specification. [46]	Y	63 MeV	3.75x10 ¹¹
MAX5069	Maxim	LDC NA; 13-059	Pulse Width Modulator	BiCMOS	DC	The part recovered functionality after 10 minutes of annealing. The part was irradiated on an application test circuit, which contained several active components, which have greater TID tolerance than the DUT. [47]	Y	50 rad(Si)/s	20 < FF < 25
MT29F32G08ABAA AWP	Micron	1106; A536	32G Flash	NAND Flash Memory	DC	Initial functional failure occurred between 20 and 50 krad(Si). All parts failed after 100 krad(Si). The failures result in an inability to perform block erase. [48]	N	50 rad(Si)/s	20 < FF < 50
SNJ54LVC14AFK	Texas Instruments	1137B; 13-029	Hex Schmitt-Trigger Inverter	BiCMOS	DC	Parameters within specification. [49]	N	50 rad(Si)/s	>30
HMC6416	Hittite Microwave	0271; 12-083	Latched Comptator	SiGe	MJC	No parametric changes observed up to 20 krad (Si) [50]	Y	10	> 20
ADV212	Analog Devices	1216; 1220; 13-050; 13-051	Video Codec	Hybrid 0.18 uCMOS	RG	All parts functional to 50 krad(Si). Leakage current increased > 50 krad(Si). [34]	Y	56 rad(Si)/s	50

TABLE IX: SUMMARY OF LOW DOSE RATE TID TEST RESULTS (ON-GOING)

Dose rate (mrad(Si)/s) unless otherwise specified.

Part Number	Manufacturer	LDC or Wafer #; REAG ID#	Device Function	Technology	PI	Results	App. Spec (Y/N)	Dose rate (mrad(Si)/s)	Degradation Level (krad(Si)) or Proton Fluence
Operational Amplifier:									
LM124 (Ceramic DIP-14)	National Semiconductor	JM0591182; A010; A132; and A148	Operational Amplifier	Bipolar	DC	Parameters within specification.	Y	1	> 100
								0.5	> 60
LM158AJRQMLV (Ceramic DIP-8)	National Semiconductor	JM084X27; A166	Operational Amplifier	Bipolar	DC	Input bias current degradation shows dose rate sensitivity below 10 mrad(Si)/s. However parameters are within specification for all dose rates.	N	5, 1	> 100
								0.5	> 70
RH1013MH (TO-5 Metal Can)	Linear Technology	0329A; A152	Operational Amplifier	Bipolar	DC	Small levels of dose rate sensitivity in the input bias current degradation. Parameters within specification.	Y	1	> 20
								0.5	> 20
RH1013MJ8 (Ceramic DIP)	Linear Technology	0305A; A152	Operational Amplifier	Bipolar	DC	Small levels of dose rate sensitivity in the input bias current degradation. Parameters within specification.	Y	1	> 20
								0.5	> 20
RH1078MH (TO-5)	Linear Technology	0741A; A224	Operational Amplifier	Bipolar	DC	Parameters remain within post-irradiation specification.	Y	1	> 40
								0.5	> 30
RH1078W (Flatpack)	Linear Technology	0325A; A224	Operational Amplifier	Bipolar	DC	Parameters remain within post-irradiation specification.	Y	1	> 40
								0.5	> 30
RHF310 (Ceramic Flat-8)	STMicroelectronics	30849A; A256	Operational Amplifier	Bipolar	DC	Input bias current and input offset voltage within specification.	N	5	> 100
								1	> 80
								0.5	> 50

Part Number	Manufacturer	LDC or Wafer #; REAG ID#	Device Function	Technology	PI	Results	App. Spec (Y/N)	Dose rate (mrad(Si)/s)	Degradation Level (krad(Si)) or Proton Fluence
RHF43B (Ceramic Flat-8)	STMicroelectronics	30820A; A257 and A589	Operational Amplifier	Bipolar	DC	Minimal dose rate sensitivity. Parameters within specification.	N	10	> 100
								1	> 50
								0.5	> 50
Transistor:									
2N2222 (Engineering samples)	Semicoa	1001; 13-024	NPN Transistor	Bipolar	DC	Minimal degradation. All parameters within specification. [43]	N	10	>100
								1	>20
								0.5	>10
2N3811JS	Semicoa	1456; 13-063	NPN Transistor	Bipolar	DC	No bias dependence Two devices exceeded specifications after 30 krad(Si).	N	50 rad(Si)/s	30 < h _{FE} < 50
								10	>15
2N3811UX	Semicoa	1994; 13-064	NPN Transistor	Bipolar	DC	Flatpack devices show slightly worse degradation than TO can packaged devices in general.	N	50 rad(Si)/s	50 < h _{FE} < 70
2N2222AJSR	Semicoa	1364; 13-017	Transistor	Bipolar	DC	LDR EF = 3.9 after 100 krad(Si).	N	10	35 < h _{FE} < 45
								5	65 < h _{FE} < 90
								1	>15
								0.5	>10
2N2907	Semicoa	0932; 13-023	PNP Transistor	Bipolar	DC	Low dose rate testing in progress. LDR EF = 1.78 after 100 krad(Si).	N	10	40 < h _{FE} < 50
2N2857	Semicoa	1008; A538	NPN Transistor	Bipolar	DC	All parameters within specification up to 100 krad(Si). Minimal LDR sensitivity.	N	50	>100
								10	> 100
2N2369	Semicoa	1934; A543, and 13-020	NPN Transistor	Bipolar	DC	All parameters within specification up to 100 krad(Si). Minimal LDR sensitivity.	N	50 rad(Si)/s, 10	> 100
2N3700JV	Semicoa	1109; A544, and 13-022	NPN Transistor	Bipolar	DC	Strong bias dependence. Biased devices show enhanced degradation than grounded devices.	N	10	20 < h _{FE} < 35
								5	25 < h _{FE} < 35
								1	>17
								0.5	>8
2N3700UBJV	Semicoa	J1935; 13-021	Transistor	Bipolar	DC	Dose rate effect not evident at this stage	N	10	10 < h _{FE} < 20
								1	>15
2N5153	Semicoa	1013; 13-019	PNP Transistor	Bipolar	DC	Minimal LDR EF.	N	1	> 30
2N5154	Semicoa	1023; 13-018	Transistor	Bipolar	DC	Minimal LDR EF.	N	1	> 30
Voltage Reference/ Voltage Regulators:									
LM136AH2.5QMLV (3-lead TO-46)	National Semiconductor	200746K019; A164	Voltage Reference	Bipolar	DC	Exhibits no LDR enhancement.	N	5, 1	> 100
								0.5	>70
LM317KTTR	Texas Instruments	0608; A113	Positive Voltage Regulator	Bipolar	DC	Parameters within specification. Observed LDR sensitivity for parts irradiated at 0.5 and 1 mrad(Si)/s after 20 krad(Si).	N	5, 1	> 100
								0.5	> 70
LT1009IDR	Texas Instruments	0606; A327	Internal Reference	Bipolar	DC	Parameters within specification. Parts exhibit minimal LDR enhancement.	N	5, 1	> 100
								0.5	> 70
RHFL4913ESY332 (TO257)	STMicroelectronics	30828A A258 and A259	Voltage Regulator	Bipolar	DC	All parameters within specification. Minimal dose rate sensitivity.	N	10, 5, 1	>100
								0.5	> 30
RHFL4913KP332 (Flat-16)	STMicroelectronics	30814B A258 and A259	Voltage Regulator	Bipolar	DC	All parameters within specification. Minimal dose rate sensitivity.	N	10, 5, 1	>100
								0.5	> 30

Part Number	Manufacturer	LDC or Wafer #; REAG ID#	Device Function	Technology	PI	Results	App. Spec (Y/N)	Dose rate (Mrad(Si)/s)	Degradation Level (krad(Si)) or Proton Fluence
Miscellaneous:									
LM139AWRQMLV	National Semiconductor	JM046X13; A009 and A095	Comparator	Bipolar	DC	Parameters within specification.	Y	0.5	> 30
TL750M05CKTRR (TO263-3)	Texas Instruments	0707; A112	LDO Positive Voltage Regulator	Bipolar	DC	One part irradiated at 1 Mrad(Si) exceeded specification at 40 krad(Si). Vout specification for full temperature range. (Characterization performed in DC mode.) Minimal dose rate sensitivity.	N	5	> 100
								1	$30 < V_{out} < 40$
								0.5	> 70

IV. TEST RESULTS AND DISCUSSION

As in our past workshop compendia of NASA Goddard Space Flight Center (GSFC) test results, each DUT has a detailed test report available online at <http://radhome.gsfc.nasa.gov> [11].

A. Aeroflex ACT4468 Transceiver SEE Test Results

The ACT4468 is a dual transceiver manufactured by Aeroflex Plainview. We irradiated three devices with 15 MeV/amu heavy ions at TAMU. The devices were biased with $V_{cc} = 5\text{ V}$. The input signal was a square wave, with V_{IL} of 0.4 V and V_{IH} of 2.7 V, a frequency of 200 kHz, and a duty cycle of 50%.

Fig. 1 shows SET cross sections as a function of effective LET for the different trigger conditions. Here, TX is the transceiver output and RX is the receiver output. We applied a pulse width trigger of 200 ns at the 0 V threshold. The error bars indicate the Poisson error at 95% confidence level. The error bars are not visible in cases where the data points are graphically larger than the error.

The receiver (RX) configuration was most susceptible to SETs, with an $2.8 < LET_{th} < 4.0\text{ MeV}\cdot\text{cm}^2/\text{mg}$, for an oscilloscope trigger set at 1 V. The SETs are typically high to low or low to high signal distortions that affect half a clock cycle as shown in Fig. 2. Here, the oscilloscope is triggering on the transceiver output. Refer to the test report for additional details [13].

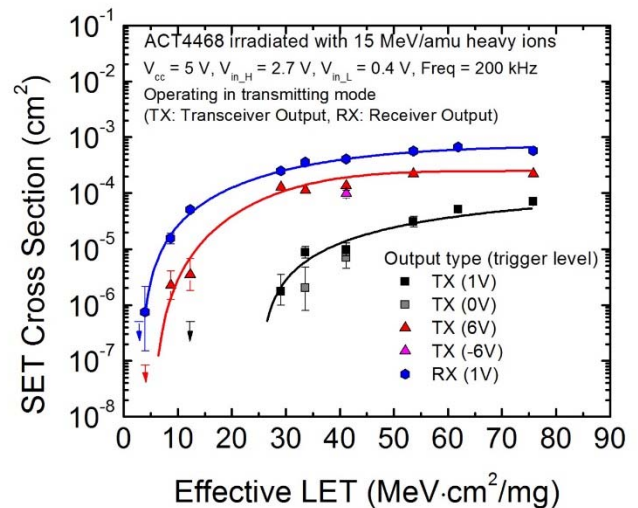


Fig. 1. SET cross sections as a function of effective LET for the different trigger conditions.

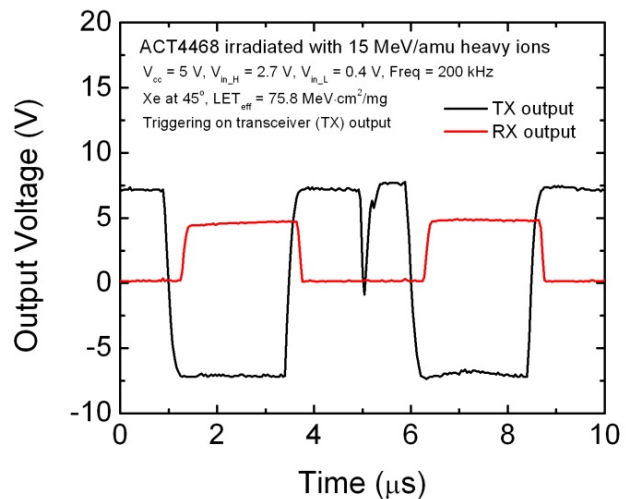


Fig. 2. Examples of a SET.

B. Analog Devices AD648 Operational Amplifier TID Test Results

The AD648 is a matched pair of low power, precision monolithic operational amplifiers that offers both low bias current and low quiescent current. Twenty parts (LDC 1225) were irradiated at a rate of 10 mrad(Si)/s with gamma rays at GSFC’s Radiation Effects Facility to a final dose of 100 krad(Si). Ten of the samples were irradiated with all pins grounded (unbiased), while the other ten were biased with ±15 V on the power supply rails, +5 V on the non-inverting inputs, and the inverting input shorted to the output with a 1 kΩ resistor to ground. An additional two parts were not irradiated, and served as control parts.

For all parameters measured, the greatest amount of degradation was observed in the parts irradiated with all pins grounded. All parameters remained within specification to 20 krad(Si), but the input bias current and open loop gain exceeded their specifications (20 pA and 300 mV/V, respectively) between 20 and 30 krad(Si). Fig. 3 shows the input bias current as a function of dose. Likewise, Fig. 4 shows the open loop gain as a function of dose.

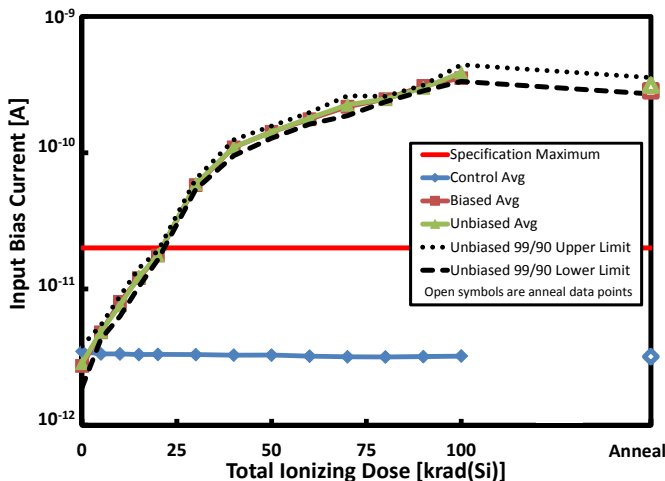


Fig. 3. The AD648 input bias current exceeds the specification of 20 pA between 20 and 30 krad(Si).

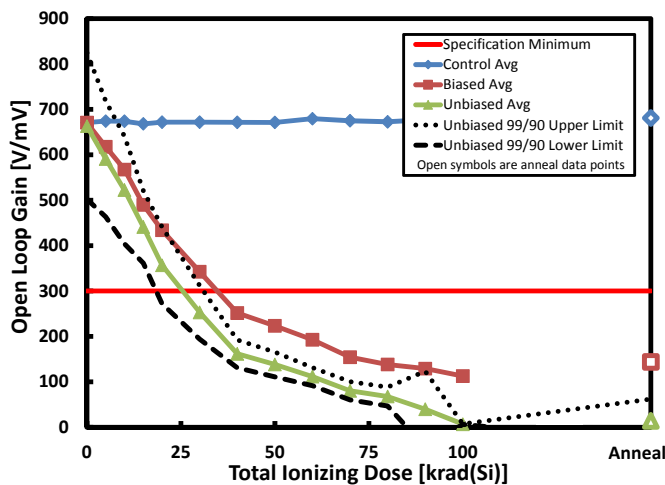


Fig. 4. AD648 open loop gain as a function of dose.

During the slew rate measurements, a large amount of ringing began appearing when the output was switching from

low to high in the unbiased parts between the 30 krad(Si) and 40 krad(Si) dose points. The output of one of unbiased amplifiers in the slew rate test circuit can be seen in Fig. 5. At each dose step after 40 krad(Si), the ringing continued to worsen in the unbiased parts, and the biased parts also began to show the same characteristics. At 80 krad(Si), the ringing became rail-to-rail, never attenuated, and the slew rate was impossible to measure. After 100 krad(Si), several of the irradiated parts from the unbiased group were tested in the engineering boards, but they were nonfunctioning. Fig. 6 shows an oscilloscope capture of the output of one of the unbiased samples with no resistive load on the output, while Fig. 7 shows the same thing but with a 10 kΩ load on the output.

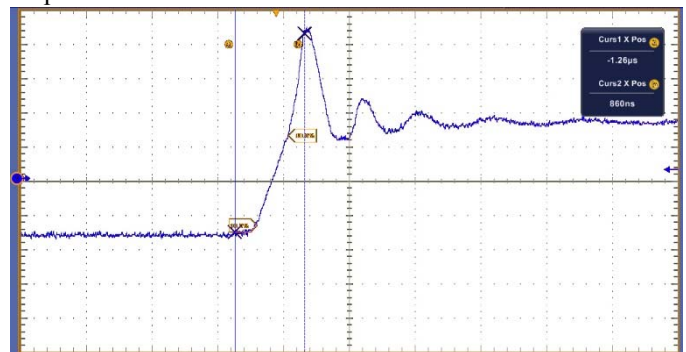


Fig. 5. Oscilloscope display when measuring the slew rate of one of the unbiased AD648s with no load connected to the output at the 40 krad(Si) dose step.

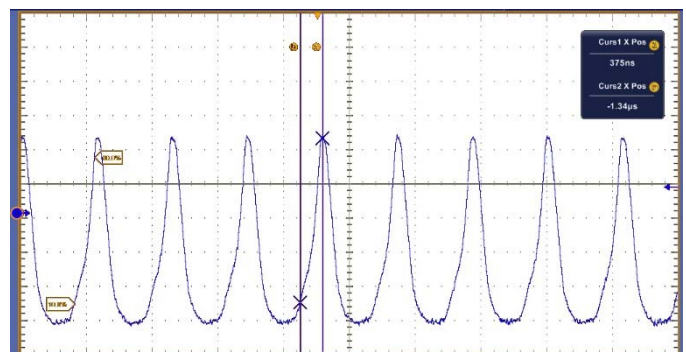


Fig. 6. Oscilloscope display when measuring the slew rate of one of the unbiased AD648s with no load connected to the output at the 100 krad(Si) dose step.

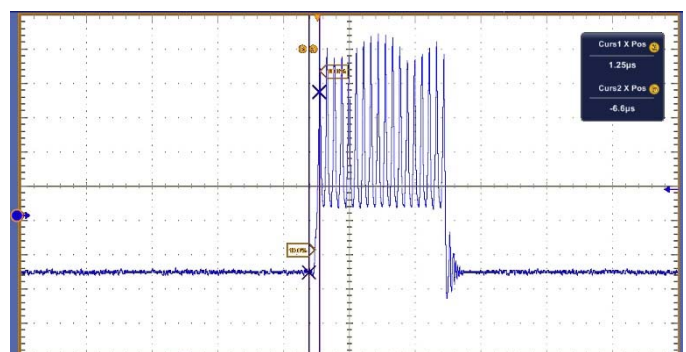


Fig. 7. Oscilloscope display when measuring the slew rate of one of the unbiased AD648s with a 10 kΩ resistor connected to the output at the 100 krad(Si) dose step.

These parts should be used with caution in environments that expect to see total doses higher than 30 or 40 krad(Si). Lot-specific testing is recommended in those situations.

C. Analog Devices OP497 Operational Amplifier TID Test Results

The OP497 is a precision picoampere input current quad operational amplifier (op amp). Three devices in an application-specific bias condition were irradiated at a rate of 10 mrad(Si)/s with a ^{60}Co gamma ray source.

All parameters remained within specifications up to 4.5 krad(Si) after which input offset current on one device exceeded specifications (150 pA) at the 7 krad(Si) reading. Fig. 8 shows the degradation due to exposure with the specification represented by a dashed line. Provided that the electrical design can sustain operation with this level of degradation, the part can be deemed usable in the application after low dose irradiation to 20 krad(Si).

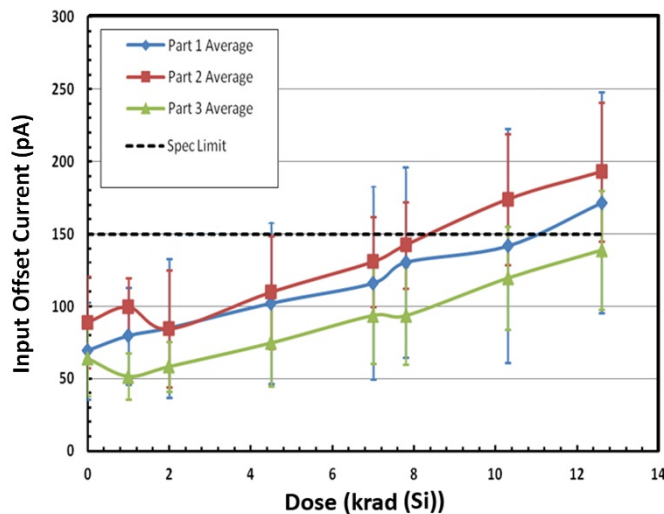


Fig. 8. Average Offset Current of OP497 parts at V_{CM} of 0 V.

V. ACKNOWLEDGMENT

The authors gratefully acknowledge supported from the NASA Electronic Parts and Packaging Program (NEPP), NASA Flight Projects, and the Defense Threat Reduction Agency (DTRA). Special thanks to members of the Radiation Effects and Analysis Group who contributed to the test results presented here: Hak Kim, Anthony M. Phan, Donald K. Hawkins, James D. Forney, Christina M. Seidleck, Martin A. Carts, Marco A. Figueiredo, and Stephen R. Cox.

VI. SUMMARY

We have presented current data from SEE, TID, and DD testing on a variety of mainly commercial devices. It is the authors' recommendation that these data be used with caution. We also highly recommend that lot testing be performed on any suspect or commercial device.

VII. REFERENCES

- [1] Kenneth A. LaBel, Lewis M. Cohn, and Ray Ladbury, "Are Current SEE Test Procedures Adequate for Modern Devices and Electronics Technologies?," http://radhome.gsfc.nasa.gov/radhome/papers/HEART08_LaBel.pdf
- [2] Michael B. Johnson, Berkeley Lawrence Berkeley National Laboratory (LBNL), 88-Inch Cyclotron Accelerator, Accelerator Space Effects (BASE) Facility <http://cyclotron.lbl.gov>.
- [3] B. Hyman, "Texas A&M University Cyclotron Institute, K500 Superconducting Cyclotron Facility," <http://cyclotron.tamu.edu/ref/>, Jul. 2003.
- [4] W.J. Stapor, "Single-Event Effects Qualification," IEEE NSREC95 Short Course, sec. II, pp 1-68, Jul. 1995.
- [5] J. S. Melinger, S. Buchner, D. McMorrow, T. R. Weatherford, A. B. Campbell, and H. Eisen, "Critical evaluation of the pulsed laser method for single event effects testing and fundamental studies," IEEE Trans. Nucl. Sci., vol 41, pp. 2574-2584, Dec. 1994.
- [6] D. McMorrow, J. S. Melinger, and S. Buchner, "Application of a Pulsed Laser for Evaluation and Optimization of SEU-Hard Designs," IEEE Trans. Nucl. Sci., vol 47, no. 3, pp. 559-565, Jun. 2000.
- [7] C. M. Castaneda, University of California at Davis (UCD) "Crocker Nuclear Laboratory (CNL) Radiation Effects Measurement and Test Facility," IEEE NSREC01 Data Workshop, pp. 77-81, Jul. 2001.
- [8] JEDEC Government Liaison Committee, Test Procedure for the Management of Single-Event Effects in Semiconductor Devices from Heavy Ion Irradiation," JESD57, <http://www.jedec.org/standards-documents/docs/jesd-57>, Dec. 1996.
- [9] Department of Defense "Test Method Standard Microcircuits," MIL-STD-883 Test Method 1019.8 Ionizing radiation (total dose) test procedure, <http://www.dscc.dla.mil/Downloads/MilSpec/Docs/MIL-STD-883/std883.pdf>, Mar. 2014.
- [10] R. Koga and W. A. Kolasinski, "Heavy Ion-Induced Single Event Upsets of Microcircuits; A Summary of the Aerospace Corporation Test Data," IEEE Trans. Nucl. Sci., vol. 31, pp. 1190 – 1195, Dec. 1984.
- [11] NASA/GSFC Radiation Effects and Analysis home page, <http://radhome.gsfc.nasa.gov>
- [12] NASA Electronic Parts and Packaging (NEPP) web site, <http://nepp.nasa.gov/>.
- [13] Dakai Chen, Ted Wilcox, Hak Kim, and Rob Davies, "Heavy ion Test Report for the ACT4468 Transceiver", 13-039_T20130507_ACT4468.pdf, May 2013.
- [14] Dakai Chen, Hak Kim, and Rob Davies, "Heavy ion Test Plan for the 54LVC14 Hex Schmitt-Trigger Inverter," 13-029_T20130506_54LVC14.pdf, May 2013.
- [15] J.-M. Lauenstein, Megan C. Casey, A.D. Topper, and E.P. Wilcox, "Single-Event Effect Testing of the GeneSiC GB20SLT12 Commercial 1200V Silicon Carbide Schottky Diode," 13-032_T20130615_GeneSiC_GB20SLT12.pdf, Jun. 2013.
- [16] J.-M. Lauenstein, Megan C. Casey, A.D. Topper, and E.P. Wilcox, "Single-Event Effect Testing of the CREE C4D40120D Schottky Diode," 13-033_C4D40120D_T20130501.pdf, May 2013.
- [17] Megan C. Casey, J.-M. Lauenstein, A. D. Topper, E. P. Wilcox and A. M. Phan, "Single-Event Effect Testing of the CREE, Inc. CPM2-1200-0025B Silicon Carbide Power MOSFET," 13-069_LBNL20130914_CREE_CPM2-1200-0025B.pdf, Sept. 2013.
- [18] M.C. Casey, J.-M. Lauenstein, E.P. Wilcox, and A.M. Phan, "Single-Event Effects Testing of the CREE, Inc. 1200 V, 80A Silicon Carbide Power MOSFET Packaged by MSKennedy as the MSK1852P," 13-070_LBNL20130914_MSK1852P.pdf, Sept. 2013.
- [19] M.C. Casey, J.-M. Lauenstein, E.P. Wilcox, and A.M. Phan, "Single-Event Effects Testing of the CREE, Inc. 1200 V, 50A Generation 2.0 Silicon Carbide Power MOSFET Packaged by MSKennedy," 13-071_LBNL20130914_CREE_MSK1852PN.pdf, Sept. 2013.
- [20] M.C. Casey, J.-M. Lauenstein, "Single-Event Effects Testing of the Infineon IDW40G65C5FKSA1 Schottky Diode," 13-038_T20130501_IDW40G65C5FKSA1.pdf, May 2013.
- [21] J.-M. Lauenstein, Megan C. Casey, A.D. Topper, and E.P. Wilcox, "Single-Event Effect Testing of the Infineon IPW65R019C7 Commercial 650V n-Type Superjunction Power MOSFET," 13-060_T20130615_IPW65R019C7.pdf, Jun. 2013.
- [22] J.-M. Lauenstein, "Single-Event Effect Testing of the FUJI MOS-250-2 MOSFET," 13-061_LBNL20130915_MOS-250-2.pdf, Sept. 2013.

- [23] M.C. Casey, J.-M. Lauenstein, and E.P. Wilcox, "Single-Event Effect Testing of the IXYS IXDI630CL Commercial MOSFET Gate Driver," 13-034_T20130601_IXDI630CL.pdf, June 2013.
- [24] M.C. Casey, J.-M. Lauenstein, and E.P. Wilcox, "Single-Event Effect Testing of the Analog Devices ADUM3223ARZ Commercial Half-Bridge Driver," 13-031_T20130506_ADUM3223AR7.pdf, May 2013.
- [25] Raymond Ladbury, "Samsung K4T1G084QF-BCE6 DDR2 SDRAM Heavy-Ion Single-Event Effects Characterization Report," 12-036_20120910_NRL20140114_DDR2.pdf, Jan. 2014.
- [26] Raymond Ladbury, "Samsung K4B2G0846-HCH9 DDR3 SDRAM Heavy-Ion Single-Event Effects Characterization Report," 13-015_12-037_T20130320_NRL20130507_DDR3.pdf, Mar. and May 2013.
- [27] Dakai Chen, Edward Wilcox, and Hak Kim, "Heavy Ion Test Report for the Panasonic MN101L Microcontroller with Embedded ReRAM," 13-075_T20131219_MN101L.pdf, Dec. 2013.
- [28] M.C. Casey, E.P. Wilcox, A. Topper, H. Kim, "Single Event Testing of Schottky Diodes," T2013May-June_SchottkyDiodeSi.pdf, May-June 2013.
- [29] Melanie D. Berg, Kenneth A. LaBel, and Jonathan A. Pellish, "Xilinx Virtex-5QV (V5QV) Independent SEU Data," presented at the NASA Electronic Parts and Packaging (NEPP) Electronics Technology Workshop, Greenbelt, MD, June 2014.
- [30] Melanie D. Berg, Hak S. Kim, Anthony M. Phan, Christina M. Seidleck, Kenneth A. LaBel, "Independent Single Event Upset Testing of the Xilinx V5QV." presented at the Single Event Effects (SEE) Symposium and the Military and Aerospace Programmable Logic Devices (MAPLD) Workshop, La Jolla, CA, May, 2014.
- [31] Melanie Berg, Ken LaBel, Hak Kim, Christina Seidleck, and Anthony Phan, "An Analysis of Heavy-Ion Single Event Effects for a Variety of Finite State-Machine Mitigation Strategies," to be presented at the Institute of Electrical and Electronics Engineers (IEEE) Nuclear and Space Radiation Effects Conference (NSREC) Paris, France, July 2014.
- [32] Dakai Chen, Hak Kim, and Rob Davies, "Heavy ion Test Report for the IS2981 Source Driver," 13-043_T20130506_IS2981.pdf, May 2013.
- [33] Megan Casey, Edward Wilcox, and Michael Xapsos, "Single-Event Transient Testing of the Texas Instruments LM6172 Dual Voltage Feedback Amplifier," 13-076_T20131218_LM6172.pdf, Dec. 2013.
- [34] Robert A. Gigliuto, "ADV212 Radiation Testing," 13-050_13-051_13-052_13-053_T20130615_VdG20130520_ADV212, May-Jun. 2013.
- [35] Kenneth P. Rodbell, Kevin G. Stawiasz, Michael S. Gordon, Phil Oldiges, Keunwoo Kim, Conal E. Murray, John G. Massey, Larry Wissel, and Henry H. K. Tang, "Single Event Transients in 32 nm SOI Stacked Latches" to be published in *IEEE Trans. on Nucl. Sci.*, Dec. 2014.
- [36] Jonathan A. Pellish, Kenneth A. LaBel, Paul W. Marshall, Kenneth P. Rodbell, Michael S. Gordon, James R. Schwank, Carlos M. Castaneda, Melanie D. Berg, Hak S. Kim, Anthony M. Phan, Christina M. Seidleck, "Criticality of Low-Energy Protons in Single-Event Effects Testing of Highly-Scaled Technologies," to be published in *IEEE Trans. on Nucl. Sci.*, Dec. 2014.
- [37] Megan Casey, "AD648 Dual Precision Operational Amplifier Total Ionizing Dose Characterization Report," 13-005_20130711_AD648_TID.pdf, Jul. 2013.
- [38] Ray Ladbury, "Total Ionizing Dose Testing of the ADI OP471 Operational Amplifier," 13-010_VdG20130403_OP471_TID.pdf, Apr. 2013.
- [39] Ray Ladbury, "Total Ionizing Dose Testing of the ADI OP484 Operational Amplifier," 12-072_VdG20121115to20130108_OP484_TID, Feb. 2013.
- [40] Michael J. Campola, "OP497 Analog Devices Operational Amplifier TID test report," 13-041_VdG20130418_OP497_TID.pdf, Apr. 2013.
- [41] Dakai Chen and Alyson Topper, "Total Ionizing Dose Test Report for the SFT2369 NPN Bipolar Junction Transistor," 13-028_VdG20120422_2N2369A_TID.pdf, July 2013.
- [42] Dakai Chen and James Forney, "Total Ionizing Dose Test Report for the SFT2907A PNP Bipolar Junction Transistor," 13-027_VdG20130422_2N2907A_TID.pdf, Apr. 2013.
- [43] Dakai Chen and James Forney, "Total Ionizing Dose Test Report for the SFT2222A NPN Bipolar Junction Transistor," 13-026_VdG20130422_SFT2222A_TID.pdf, Apr. 2013.
- [44] Michael J. Campola, "M/A-COM SMA1031 Amplifier TID test report," 12-051_VdG20130709_SMA1031_TID.pdf, July 2013.
- [45] T. Wilcox and M. Campola, "Total Ionizing Dose Test Report: ON Semiconductor NB7L14MN Differential 1:4 Fanout Buffer," 12-055_VdG20130313_NB7L14MN_TID.pdf, Mar. 2013.
- [46] Michael J. Campola, "Cypress Semiconductor STAR1000 CCD Image Sensor Displacement Damage Testing at UDC," 13-042_D20130422_SMA1031.pdf, Apr. 2013.
- [47] Dakai Chen, Ted Wilcox, Mike Xapsos, and Jonathan Pellish, "Total Dose Test Report for the MAX5069A Pulse Width Modulator Controller," 13-059_MAX5069_VdG20130611_TID.pdf, Jun. 2013.
- [48] Dakai Chen, "Total Dose Test Report for the Micron 32G NAND Flash Nonvolatile Memory," A536_VdG20130304_MT29F32G08ABAAA_WP_32Gflash_TID.pdf, Mar. 2013.
- [49] Dakai Chen and James Forney, "Total Ionizing Dose Test Report for the SN54LVC14A Inverter," 13-029_VdG20130805_SN54LVC14A_TID.pdf, Aug. 2013.
- [50] T. Wilcox and M. Campola, "Total Ionizing Dose Test Report: Hittite Microwave HMC6416USLC3 10 GHz Comparator," 12-083_VdG20130617_HMC6416_TID.pdf, Jun. 2013.